Kinetic stability properties of nonrelativistic non-neutral electron flow in a planar diode with applied magnetic field

Ronald C. Davidson
Plasma Fusion Center, Massachusetts Institute of Technology, Cambridge, Massachusetts 02139

Han S. Uhm
Naval Surface Weapons Center, Silver Spring, Maryland 20910

(Received 19 October 1984)

The linearized Vlasov-Poisson equations are used to investigate the electrostatic stability properties of nonrelativistic non-neutral electron flow in a planar diode with cathode located at $x=0$ and anode at $x=d$. The electron layer is immersed in a uniform applied magnetic field $B_0\hat{e}_z$, and the equilibrium flow velocity $V_{yb}^0(x)$ is in the y direction. Stability properties are calculated for perturbations about the choice of self-consistent Vlasov equilibrium $f_b^0(H,P_y)=(\hat{n}_b/2\pi m)\delta(H)\delta(P_y)$, which gives an equilibrium with uniform electron density ($\hat{n}_b=$const) extending from the cathode ($x=0$) to the outer edge of the electron layer ($x=x_b$). Assuming flute perturbations ($\partial/\partial z=0$) of the form $\delta\phi(x,y,t)=\delta\hat{\phi}_k(x)\exp(iky-i\omega t)$, the eigenvalue equation for $\delta\hat{\phi}_k(x)$ is simplified and solved analytically for long-wavelength, low-frequency perturbations satisfying $kx_b\ll 1$ and $|\omega-kV_d|^2\ll\omega_v^2\equiv\omega_c^2-\hat{\omega}_{pb}^2$. This gives a quadratic dispersion relation for the complex oscillation frequency ω. Defining $\mu=\hat{\omega}_{pb}^2/\omega_v^2$ and $g=d/(d-x_b)$, it is shown that the necessary and sufficient condition for instability ($\mathrm{Im}\omega>0$) is given by $(1+\mu+g)(\mu+g)>2(1+\mu)(1+\mu/4)^2$. It is found that the maximum growth rate in the unstable region can be substantial. For example, for $d=2x_b$ and $g=2$, the maximum growth rate is $(\mathrm{Im}\omega)_{\max}\simeq 0.25(kx_b)\omega_c$, which occurs for $\mu\simeq 2.3$.

I. INTRODUCTION AND SUMMARY

There is considerable interest in the equilibrium and stability properties of sheared, non-neutral electron flow in cylindrical[1,2] and planar[3–7] models of high-voltage diodes with applications to the generation of intense charged-particle beams for inertial confinement fusion.[8,9] These analyses[1–7] have represented major extensions of earlier work[9–15] to include the important influence of cylindrical,[1,2] nonlinear,[3] relativistic,[2,4–7] electromagnetic,[4–7] and kinetic[2,5] effects on equilibrium and stability behavior. The majority of these studies, however, have been based on a macroscopic cold-fluid description of the electron flow. While such models provide important insights into gross stability properties, they are not readily generalized to incorporate the important influence of kinetic effects that depend on the detailed features of the electron distribution function $f_b(\mathbf{x},\mathbf{p},t)$. The present analysis makes use of the linearized Vlasov-Poisson equations to investigate electrostatic stability properties of nonrelativistic electron flow in a planar diode with uniform applied magnetic field $B_0\hat{e}_z$. Such a model of course incorporates kinetic and finite-temperature effects in a natural manner. Moreover, many of the theoretical techniques used here have been developed in earlier studies[14–20] of the kinetic equilibrium and stability properties of non-neutral plasmas, appropriately extended to planar diode geometry.

In the present analysis, we make use of the linearized Vlasov-Poisson equations to investigate the electrostatic stability properties of nonrelativistic non-neutral electron flow in a planar diode. As illustrated in Fig. 1, the cathode is located at $x=0$ and the anode is located at $x=d$. Moreover, the electron layer is immersed in a uniform applied magnetic field $B_0\hat{e}_z$, and the equilibrium electron flow velocity $V_{yb}^0(x)$ is in the y direction. The basic assumptions and kinetic equilibrium model are described in Sec. II, and detailed equilibrium properties are calculated for the specific choice of self-consistent Vlasov equilibrium $f_b^0(H,P_y)=(\hat{n}_b/2\pi m)\delta(H)\delta(P_y)$. Here, $H=(2m)^{-1}(p_x^2+p_y^2+p_z^2)-e\phi_0(x)$ is the electron energy, $P_y=p_y-m\omega_c x$ is the canonical momentum in the y direction, $\phi_0(x)$ is the equilibrium electrostatic potential, and $\omega_c=eB_0/mc$ is the electron cyclotron frequency. This choice of $f_b^0(H,P_y)$ leads to a uniform density pro-

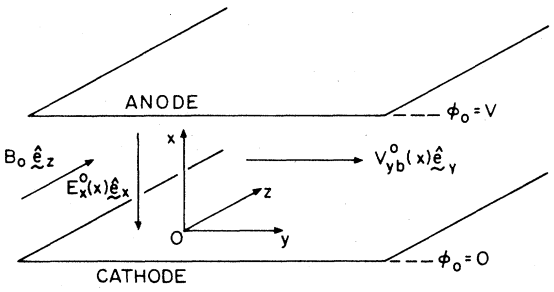

FIG. 1. Planar diode configuration and Cartesian coordinate system.

file $n_b^0(x)=\hat{n}_b=$const over the interval $0\le x<x_b \equiv -2eE_c/m\omega_v^2$ [Eq. (19) and Fig. 2], and a parabolic temperature profile $T_{\perp b}^0(x)$ that assumes its maximum value $\hat{T}_{\perp b}=(m/8)\omega_v^2 x_b^2$ at $x=x_M\equiv x_b/2$ [Eq. (25) and Fig. 2]. Here, $E_c=-(\partial\phi_0/\partial x)_{x=0}$ is the electric field at the cathode; $\omega_v^2\equiv\omega_c^2-\hat{\omega}_{pb}^2$ (assumed positive) is the square of the frequency of oscillations in the (x',y') orbits including the influence of the self-electric field $E_x^0(x)\hat{\mathbf{e}}_x$ and applied magnetic field $B_0\hat{\mathbf{e}}_z$; and $\hat{\omega}_{pb}^2=4\pi\hat{n}_b e^2/m$ is the plasma frequency squared.

In Sec. III, the linearized Vlasov-Poisson equations are used to investigate electrostatic stability properties for flute perturbations ($\partial/\partial z=0$) about the general class of self-consistent planar Vlasov equilibria $f_b^0(H,P_y)$. This leads to the eigenvalue equation for the perturbed potential amplitude $\delta\hat{\phi}_k(x)$ given in Eq. (38). The particle trajectories (x',y') are then calculated for the specific choice of equilibrium distribution function $f_b^0(H,P_y)=(\hat{n}_b/2\pi m)\delta(H)\delta(P_y)$ in Eq. (14) and the corresponding rectangular density profile in Eq. (19). For this choice of f_b^0, the exact eigenvalue equation (38) reduces to Eq. (54).

In Sec. IV, the eigenvalue equation (54) is simplified and solved analytically for low-frequency, long-wavelength perturbations satisfying $|\omega-kV_d|\ll\omega_v$, and $kx_M\ll 1$. Here $V_d\equiv V_{yb}^0(x_M)=\omega_c x_M$, where $x_M=x_b/2$. Since $\omega_v^2=\omega_c^2-\hat{\omega}_{pb}^2>0$ is assumed, the present stability analysis is restricted to densities below Brillouin flow (i.e., $\hat{\omega}_{pb}^2<\omega_c^2$). We adopt a model in which all oscillatory contributions to the orbits x_0' and y_0' in Eqs. (55) and (56) are neglected [see Eqs. (51) and (52)]. These terms generally give rise to harmonic contributions to the exponent in the orbit integral (55) of the form $\omega-kV_d-n\omega_v$ for $n\neq 0$, as well as a modification of the amplitude of the $n=0$ term in the orbit integral proportional to $(\omega-kV_d)^{-1}$. Specifically, in order to investigate the qualitative features of stability properties for $|\omega-kV_d|\ll\omega_v$ and $kx_M\ll 1$, the model approximates $y_0'=y+V_d\tau$, $x_0'=x_M$, $\delta\hat{\phi}_k(x_0')=\delta\phi_k(x_M)$, and $(\partial/\partial x_0')\delta\hat{\phi}_k(x_0')=[\partial\delta\phi_k(x)/\partial x]_{x=x_M}$ in Eqs. (55) and (56). This gives the approximate eigenvalue equation (65). In Sec. IV C, the eigenvalue equation (65) is solved exactly for long-wavelength perturbations with $kx_M\ll 1$, and it is shown that the resulting dispersion relation for the complex eigenfrequency ω is given by [Eq. (77)]

$$(g+\mu)\left[\frac{\omega-kV_d}{kV_d}\right]^2+2\mu\left[1+\frac{1}{4}\mu\right]\left[\frac{\omega-kV_d}{kV_d}\right]+\frac{1}{2}\frac{\mu^2}{1+\mu}(1+\mu+g)=0\,,$$

where the geometric factor g is defined by $g=d/(d-x_b)$. The necessary and sufficient condition for instability ($\mathrm{Im}\omega>0$) is given by

$$\frac{1}{2}\frac{(1+\mu+g)(\mu+g)}{1+\mu}>\left[1+\frac{1}{4}\mu\right]^2.$$

Moreover, in the unstable region of (μ,g) parameter space, the growth rate $\mathrm{Im}\omega$ can be expressed as [Eq. (83)]

$$\frac{\mathrm{Im}\omega}{kV_d}=\frac{\mu}{g+\mu}\left[\frac{1}{2}(g+\mu)\left[1+\frac{g}{1+\mu}\right]-\left[1+\frac{\mu}{4}\right]^2\right]^{1/2},$$

where $kV_d>0$ is assumed. It is found that the maximum growth rate for the instability can be substantial. For example, for $d=2x_b$ and $g=2$, maximum growth occurs for $\mu\simeq 2.3$, with $(\mathrm{Im}\omega)_{\max}\simeq 0.5kV_d=0.5(kx_M)\omega_c$.

Finally, the present analysis has important implications for stable diode operation, at least with regard to the low-frequency, long-wavelength flute perturbations considered here. These implications are discussed in Sec. V.

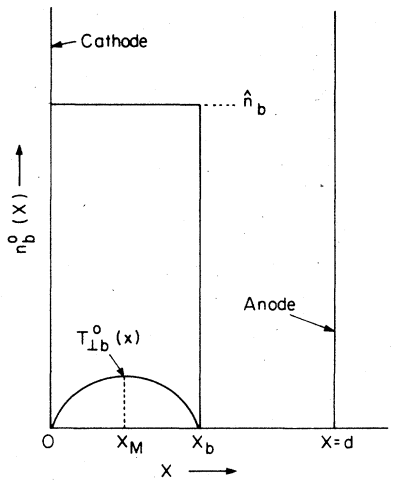

FIG. 2. Equilibrium density profile $n_b^0(x)$ [Eq. (19)] and temperature profile $T_{\perp b}^0(x)$ [Eq. (25)] for the choice of distribution function f_b^0 in Eq. (14).

II. ASSUMPTIONS AND KINETIC EQUILIBRIUM MODEL

A. Assumptions

In the present analysis we make use of the Vlasov-Poisson equations to investigate the electrostatic stability properties of nonrelativistic non-neutral electron flow in a planar diode. The diode configuration is illustrated in Fig. 1 where the cathode is located at $x=0$ and the anode at $x=d$. The non-neutral electron plasma is immersed in a uniform applied magnetic field $B_0\hat{\mathbf{e}}_z$, and the average electron flow is in the y direction. To make the analysis tractable, the following simplifying assumptions are made.

(a) Perturbations are about a quasisteady equilibrium ($\partial/\partial t=0$) with no spatial variation in the y and z directions, i.e., $\partial/\partial y=0=\partial/\partial z$. However, equilibrium quantities are allowed to vary in the x direction with $\partial/\partial x\neq 0$.

(b) We denote the equilibrium electric field by $\mathbf{E}_0(\mathbf{x})=E_x^0(x)\hat{\mathbf{e}}_x$, where $E_x^0(x)=-\partial\phi_0(x)/\partial x$ and $\phi_0(x)$ is the electrostatic potential. The boundary conditions on $\phi_0(x)$ are

$$\phi_0(x=0)=0 \quad \text{and} \quad \phi_0(x=d)=V\,, \tag{1}$$

where V is the applied voltage. In general, it is assumed that the equilibrium electric field at the cathode,

$$E_c = -\left.\frac{\partial \phi_0}{\partial x}\right|_{x=0}, \tag{2}$$

is nonzero. The limiting case $E_c = 0$ corresponds to space-charge-limited flow.[4,6]

(c) For nonrelativistic electron flow, with $eV/mc^2 \ll 1$, the equilibrium electron current in the y direction, $-e\int d^3p\, v_y f_b^0(x,\mathbf{p})$, is sufficiently low that the induced axial self-magnetic field $B_{0z}^s(x)\hat{\mathbf{e}}_z$ is negligibly small in comparison with the externally applied magnetic field $B_0\hat{\mathbf{e}}_z$.[21,22]

(d) For present purposes, perturbed quantities are assumed to be independent of z ($\partial/\partial z = 0$) and spatially periodic in the y direction with periodicity length L. Perturbed quantities $\delta\psi(x,y,t)$ are expressed as

$$\begin{aligned}\delta\psi(x,y,t) &= \delta\hat{\psi}(x,y)\exp(-i\omega t) \\ &= \sum_k \delta\hat{\psi}_k(x)\exp(iky - i\omega t)\,,\end{aligned} \tag{3}$$

where $\mathrm{Im}\omega > 0$ corresponds to instability. Here, $k = 2\pi n/L$, n is an integer, and the summation $\sum_k$ extends from $n = -\infty$ to $n = +\infty$. The boundary conditions on the perturbed electrostatic potential at the cathode and the anode are

$$\delta\hat{\phi}_k(x=0) = 0 = \delta\hat{\phi}_k(x=d)\,, \tag{4}$$

which corresponds to zero tangential electric field, $\delta\hat{E}_y = -(\partial/\partial y)\delta\hat{\phi} = 0$ at $x = 0$ and at $x = d$.

B. General equilibrium properties

Any distribution function $f_b^0(x,\mathbf{p})$ that is a function only of the single-particle constants of the motion in the equilibrium field configuration is a solution to the steady-state ($\partial/\partial t = 0$) Vlasov equation.[16] For $\mathbf{E}_0(\mathbf{x}) = -\hat{\mathbf{e}}_x \partial\phi_0(x)/\partial x$ and $\mathbf{B}_0(\mathbf{x}) = B_0\hat{\mathbf{e}}_z$, the single-particle constants of the motion consistent with the assumptions in Sec. II A are the axial momentum $p_z = mv_z$, the canonical momentum in the y direction

$$P_y = p_y - m\omega_c x\,, \tag{5}$$

and the particle energy

$$H = \frac{\mathbf{p}^2}{2m} - e\phi_0(x)\,. \tag{6}$$

Here, $-e$ is the electron charge, m is the electron mass, $\omega_c = eB_0/mc$ is the electron cyclotron frequency, $\mathbf{p} = m\mathbf{v}$ is the mechanical momentum, and $\mathbf{p}^2 = p_x^2 + p_y^2 + p_z^2$. For present purposes, we consider the class of self-consistent Vlasov equilibria[16,17]

$$f_b^0(x,\mathbf{p}) = f_b^0(H,P_y) \tag{7}$$

that depend explicitly on H and P_y but not on axial momentum p_z.

For specified $f_b^0(H,P_y)$, the equilibrium electron density $n_b^0(x)$ is defined by

$$n_b^0(x) = \int d^3p\, f_b^0(H,P_y)\,, \tag{8}$$

and the electrostatic potential $\phi_0(x)$ is determined self-consistently from Poisson's equation

$$\begin{aligned}\frac{\partial^2}{\partial x^2}\phi_0(x) &= 4\pi e n_b^0(x) \\ &= 4\pi e\int d^3p\, f_b^0(H,P_y)\,.\end{aligned} \tag{9}$$

Since H depends on $\phi_0(x)$, it is evident that Eq. (9) is generally a nonlinear equation for the electrostatic potential $\phi_0(x)$. Making use of the boundary conditions in Eqs. (1) and (2), Poisson's equation (9) can be integrated to give

$$\phi_0(x) = -E_c x + 4\pi e\int_0^x dx''\int_0^{x''} dx' n_b^0(x') \tag{10}$$

in the diode region $0 \le x \le d$. Enforcing $\phi_0(x=d) = V$, the applied voltage V is related to E_c and the equilibrium density profile $n_b^0(x)$ by

$$V = -E_c d + 4\pi e\int_0^d dx''\int_0^{x''} dx' n_b^0(x')\,. \tag{11}$$

For specified $f_b^0(H,P_y)$, other equilibrium properties are also readily calculated. For example, since H is an even function of p_x and p_z, the average flow velocities in the x and z directions are trivially zero, i.e.,

$$\langle v_x\rangle = \int d^3p\, v_x f_b^0 \Big/ \int d^3p\, f_b^0 = 0\,,$$
$$\langle v_z\rangle = \int d^3p\, v_z f_b^0 \Big/ \int d^3p\, f_b^0 = 0\,.$$

On the other hand, since $f_b^0(H,P_y)$ depends explicitly on P_y, the average flow velocity in the y direction is generally nonzero. Denoting

$$V_{yb}^0(x) = \langle v_y\rangle = \int d^3p\, v_y f_b^0 \Big/ \int d^3p\, f_b^0\,,$$

the equilibrium flux of particles in the y direction is given by

$$n_b^0(x)V_{yb}^0(x) = \int d^3p\, v_y f_b^0(H,P_y)\,. \tag{12}$$

In a similar manner we can define an effective temperature $T_{\perp b}^0(x)$ perpendicular to the equilibrium flow direction by

$$n_b^0(x)T_{\perp b}^0(x) = \int d^3p\,\frac{p_x^2+p_z^2}{2m} f_b^0(H,P_y)\,. \tag{13}$$

C. Equilibrium model

For purposes of the stability analysis in Secs. III and IV, we consider electrostatic perturbations about the specific choice of equilibrium distribution function[17,18,20]

$$f_b^0(x,\mathbf{p}) = \frac{\hat{n}_b}{2\pi m}\delta(H)\delta(P_y)\,, \tag{14}$$

where $P_y = p_y - m\omega_c x$, $H = \mathbf{p}^2/2m - e\phi_0(x)$, and $\hat{n}_b$ is a constant. The choice of f_b^0 in Eq. (14) corresponds to emission of electrons from the cathode with zero kinetic energy, i.e., $(2m)^{-1}(p_x^2+p_y^2+p_z^2) = 0$ at $x = 0$. It necessarily follows that p_x, p_y, and p_z are separately equal to zero at the cathode ($x = 0$). Substituting Eq. (14) into Eq. (8) and integrating over p_y, the electron density profile $n_b^0(x)$ can be expressed as

$$n_b^0(x) = 2\hat{n}_b\int_0^\infty dp_\perp p_\perp \delta(p_\perp^2 - p_{\perp 0}^2(x))\,, \tag{15}$$

where $p_\perp^2=p_x^2+p_z^2$, and $p_{\perp 0}^2(x)=[2me\phi_0(x)-p_y^2]_{P_y=0}$ is defined by

$$p_{\perp 0}^2(x)=2me\phi_0(x)-m^2\omega_c^2x^2 . \tag{16}$$

Carrying out the integration over $p_\perp$ in Eq. (15), we obtain the rectangular density profile (Fig. 2)

$$n_b^0(x)=\begin{cases}\hat{n}_b=\text{const}, & p_{\perp 0}^2(x)\geq 0\\ 0, & p_{\perp 0}^2(x)<0 .\end{cases} \tag{17}$$

That is, the boundary ($x=x_b$) of the electron layer is determined from $p_{\perp 0}^2(x_b)=0$, or equivalently,

$$-e\phi_0(x_b)+\tfrac{1}{2}m\omega_c^2x_b^2=0 . \tag{18}$$

Note that Eq. (18) corresponds to the envelope of turning points for which $p_x^2+p_z^2=0$. The equilibrium density profile in Eq. (17) can be expressed in the equivalent form (Fig. 2)

$$n_b^0(x)=\begin{cases}\hat{n}_b=\text{const}, & 0\leq x<x_b\\ 0, & x_b<x\leq d\end{cases} \tag{19}$$

where x_b is determined self-consistently from Eq. (18).

Substituting Eq. (19) into the equilibrium Poisson equation (9), and enforcing the boundary conditions in Eqs. (1) and (2), we obtain

$$\phi_0(x)=\begin{cases}-E_cx+2\pi\hat{n}_bex^2, & 0\leq x<x_b\\ V+(4\pi\hat{n}_bex_b-E_c)(x-d), & x_b<x\leq d\end{cases} \tag{20}$$

where $E_c=-\partial\phi_0/\partial x\,|_{x=0}$. Note from Eq. (20) that $\partial\phi_0/\partial x$ is continuous at $x=x_b$. The remaining boundary condition, that the potential $\phi_0(x)$ is also continuous at $x=x_b$, determines the voltage V self-consistently in terms of other system parameters. This gives

$$V=-E_cd+4\pi e\hat{n}_bx_b(d-x_b/2) . \tag{21}$$

Substituting Eq. (20) into Eq. (18), the location of the layer boundary (x_b) is determined from

$$\tfrac{1}{2}m(\omega_c^2-\hat{\omega}_{pb}^2)x_b^2=-eE_cx_b , \tag{22}$$

where $\hat{\omega}_{pb}^2=4\pi\hat{n}_be^2/m$. The solution $x_b=0$ to Eq. (22) corresponds to the location of the cathode ($x=0$). The remaining solution for x_b corresponds to the location of the outer edge of the electron layer in Fig. 2, i.e.,

$$x_b=\frac{-2eE_c/m}{\omega_c^2-\hat{\omega}_{pb}^2} . \tag{23}$$

For present purposes, we assume $E_c\leq 0$ and densities below or at Brillouin flow, i.e., $\hat{\omega}_{pb}^2\leq\omega_c^2$. This assures $x_b>0$ in Eq. (23) and Fig. 2. The condition $x_b<d$ imposes the further restriction $-2eE_c/m<(\omega_c^2-\hat{\omega}_{pb}^2)d$. For specified $E_c<0$ and $\hat{\omega}_{pb}^2<\omega_c^2$, the boundary location x_b can be calculated self-consistently from Eq. (23). Note from Eq. (23) that the limiting case of Brillouin flow ($\hat{\omega}_{pb}^2/\omega_c^2\to 1$) corresponds to $E_c\to 0$ and $\omega_c^2-\hat{\omega}_{pb}^2\to 0$ with the ratio $E_c/(\omega_c^2-\hat{\omega}_{pb}^2)$ remaining finite.

For the choice of distribution function in Eq. (14), the average flow velocity in the y direction defined in Eq. (12) is readily shown to be

$$V_{yb}^0(x)=\omega_cx \tag{24}$$

in the region $0\leq x<x_b$ where the electron density is nonzero. On the other hand, from Eq. (20), the equilibrium $\mathbf{E}_0\times\mathbf{B}_0$ velocity, $V_E(x)=-cE_x^0(x)/B_0$, is given by $V_E(x)=-cE_c/B_0+(\hat{\omega}_{pb}^2/\omega_c)x$. The fact that $V_{yb}^0(x)$ and $V_E(x)$ are generally different is a reflection that the distribution function $f_b^0(x,\mathbf{p})$ in Eq. (14) has nonzero temperature $T_{\perp b}^0(x)$ and there is a corresponding pressure-gradient force on an electron fluid element. Making use of Eqs. (13), (14), and (23), we find that $T_{\perp b}^0(x)$ can be expressed as

$$\begin{aligned}T_{\perp b}^0(x)&=-eE_cx+\frac{m}{2}(\hat{\omega}_{pb}^2-\omega_c^2)x^2\\ &=\frac{m}{2}(\omega_c^2-\hat{\omega}_{pb}^2)(xx_b-x^2)\\ &=\frac{m}{2}(\omega_c^2-\hat{\omega}_{pb}^2)\left[\left[\frac{x_b}{2}\right]^2-\left[x-\frac{x_b}{2}\right]^2\right]\end{aligned} \tag{25}$$

for $0\leq x<x_b$. Note from Eq. (25) that $T_{\perp b}^0(x=0)=0=T_{\perp b}^0(x=x_b)$, and that $T_{\perp b}^0(x)$ assumes its maximum value $\hat{T}_{\perp b}=(m/8)(\omega_c^2-\hat{\omega}_{pb}^2)x_b^2$, at $x=x_M\equiv x_b/2$ (Fig. 2).

As a further point, it is readily verified that the equilibrium profiles in Eqs. (19), (20), (24), and (25) are consistent with equilibrium force balance on an electron fluid element, i.e.,

$$\frac{\partial}{\partial x}[n_b^0(x)T_{\perp b}^0(x)]=-n_b^0(x)e\left[E_x^0(x)+\frac{V_{yb}^0}{c}B_0\right] , \tag{26}$$

as expected.

In conclusion, an attractive feature of the choice of equilibrium distribution function $f_b^0(x,\mathbf{p})$ in Eq. (14) is that the corresponding (self-consistent) density profile has the simple rectangular form in Eq. (19) and that other equilibrium properties are equally tractable analytically [see Eqs. (20), (24), and (25)]. Although Eq. (14) necessarily implies that $p_x=p_y=p_z=0$ at the cathode ($x=0$), we note that $p_x^2+p_z^2=p_{\perp 0}^2(x)$ is generally nonzero except at $x=0$ and $x=x_b$. The exception is the limit of Brillouin flow ($E_c\to 0$ and $\hat{\omega}_{pb}^2/\omega_c^2\to 1$) where $p_{\perp 0}^2(x)=0=2mT_{\perp b}^0(x)$, and the electron flow is laminar over the entire interval $0\leq x\leq x_b$.

As is often the case, depending on the application, there is some degree of latitude in the specific choice of Vlasov equilibrium $f_b^0(x,\mathbf{p})$. For example, an alternate choice of equilibrium distribution function consistent with $p_x=p_y=p_z=0$ at the cathode ($x=0$) would be $f_b^0(x,\mathbf{p})=\text{const}\times\delta(H)\delta(P_y)\delta(p_z)$. For this choice of distribution function, however, the corresponding self-consistent density profile $n_b^0(x)=\int d^3p\,f_b^0(x,\mathbf{p})$ is singular both at $x=0$ and at $x=x_b$ [where $p_{\perp 0}^2(x_b)=2me\phi_0(x_b)-m^2\omega_c^2x_b^2=0$], and the expression for $n_b^0(x)$ no longer has the simple rectangular form in Eq. (19).

III. ELECTROSTATIC STABILITY PROPERTIES

A. Linearized Vlasov-Poisson equations

Making use of the assumptions outlined in Sec. II A, we investigate linear stability properties for electrostatic perturbations about the class of self-consistent Vlasov equilibria $f_b^0(x,\mathbf{p})=f_b^0(H,P_y)$. For two-dimensional spatial variations, the perturbed distribution function and electrostatic potential are expressed as[16]

$$\delta f_b(\mathbf{x},\mathbf{p},t)=\delta\hat{f}_b(x,y,\mathbf{p})\exp(-i\omega t)\ ,$$
$$\delta\phi(\mathbf{x},t)=\delta\hat{\phi}(x,y)\exp(-i\omega t)\ , \tag{27}$$

where $\mathrm{Im}\omega>0$ corresponds to instability. The perturbed electric field is given by $\delta\mathbf{E}(\mathbf{x},t)=-\nabla\delta\phi(\mathbf{x},t)$, and the potential amplitude $\delta\hat{\phi}(x,y)$ satisfies the linearized Poisson equation

$$\left[\frac{\partial^2}{\partial x^2}+\frac{\partial^2}{\partial y^2}\right]\delta\hat{\phi}(x,y)=4\pi e\int d^3p\,\delta\hat{f}_b(x,y,\mathbf{p})\ . \tag{28}$$

Making use of the method of characteristics, we integrate the linearized Vlasov equation from $t'=-\infty$ to $t'=t$. Neglecting initial perturbations, the formal solution for $\delta\hat{f}_b$ can be expressed as[17]

$$\delta\hat{f}_b(x,y,\mathbf{p})=e\int_{-\infty}^{t}dt'\exp[-i\omega(t'-t)]\times\delta\hat{\mathbf{E}}(\mathbf{x}')\cdot\left[\frac{\partial}{\partial\mathbf{p}}f_b^0(x,\mathbf{p})\right]_{(\mathbf{x}',\mathbf{p}')}\ , \tag{29}$$

where

$$\delta\hat{\mathbf{E}}(\mathbf{x}')=-\hat{\mathbf{e}}_x(\partial/\partial x')\delta\hat{\phi}(x',y')-\hat{\mathbf{e}}_y(\partial/\partial y')\delta\hat{\phi}(x',y')\ .$$

In Eq. (29), $\mathbf{x}'(t')$ and $\mathbf{p}'(t')$ are the particle trajectories in the equilibrium field configuration that pass through the phase-space point $(\mathbf{x},\mathbf{p})$ at time $t'=t$. That is, $\mathbf{x}'(t')$ and $\mathbf{p}'(t')=m\mathbf{v}'(t')$ satisfy

$$m\frac{d}{dt'}\mathbf{v}'(t')=-eE_x^0(x')\hat{\mathbf{e}}_x-e\frac{\mathbf{v}'(t')\times B_0\hat{\mathbf{e}}_z}{c}\ ,$$
$$\frac{d}{dt'}\mathbf{x}'(t')=\mathbf{v}'(t')\ , \tag{30}$$

subject to the "initial" conditions

$$\mathbf{x}'(t'=t)=\mathbf{x}\ ,$$
$$\mathbf{v}'(t'=t)=\mathbf{v}\ . \tag{31}$$

These trajectories are determined in closed form in Sec. III B for the choice of equilibrium distribution function $f_b^0(H,P_y)$ in Eq. (14).

Continuing with the formal simplification of Eqs. (28) and (29), we note that

$$\frac{\partial}{\partial\mathbf{p}}f_b^0(H,P_y)=\frac{\mathbf{p}}{m}\frac{\partial f_b^0}{\partial H}+\hat{\mathbf{e}}_y\frac{\partial f_b^0}{\partial P_y}\ . \tag{32}$$

Making use of

$$\mathbf{v}'\cdot\delta\hat{\mathbf{E}}(\mathbf{x}')=-\mathbf{v}'\cdot(\partial/\partial\mathbf{x}')\delta\hat{\phi}(\mathbf{x}')$$
$$=-(d/dt')\delta\hat{\phi}(\mathbf{x}')\ ,$$

and the fact that $\partial f_b^0/\partial H$ and $\partial f_b^0/\partial P_y$ are constant (independent of t') along a particle trajectory, Eq. (29) can be expressed in the equivalent form

$$\delta\hat{f}_b(x,y,\mathbf{p})=-e\frac{\partial f_b^0}{\partial H}\int_{-\infty}^{t}dt'\exp[-i\omega(t'-t)]\frac{d}{dt'}\delta\hat{\phi}(x',y')-e\frac{\partial f_b^0}{\partial P_y}\int_{-\infty}^{t}dt'\exp[-i\omega(t'-t)]\frac{\partial}{\partial y'}\delta\hat{\phi}(x',y')\ . \tag{33}$$

In Eq. (33), we Fourier decompose with respect to the y dependence [Eq. (3)], and integrate by parts the contribution proportional to $(d/dt')\delta\hat{\phi}$. This gives

$$\delta\hat{f}_{bk}(x,\mathbf{p})=-e\frac{\partial f_b^0}{\partial H}\delta\hat{\phi}_k(x)-ei\left[\omega\frac{\partial f_b^0}{\partial H}+k\frac{\partial f_b^0}{\partial P_y}\right]\int_{-\infty}^{t}dt'\exp[-i\omega\tau+ik(y'-y)]\delta\hat{\phi}_k(x') \tag{34}$$

for the kth Fourier amplitude. Here $\tau=t'-t$, and $\delta\hat{f}_{bk}(x,\mathbf{p})$ is related self-consistently to $\delta\hat{\phi}_k(x)$ by the linearized Poisson equation

$$\frac{\partial^2}{\partial x^2}\delta\hat{\phi}_k(x)-k^2\delta\hat{\phi}_k(x)=4\pi e\int d^3p\,\delta\hat{f}_{bk}(x,\mathbf{p})\ . \tag{35}$$

Substituting Eq. (34) into Eq. (35) then gives a closed eigenvalue equation that can be used to determine the eigenfunction $\delta\hat{\phi}_k(x)$ and complex eigenfrequency ω for electrostatic perturbations about the general equilibrium distribution function $f_b^0(H,P_y)$. We note that the orbit integral[17]

$$I\equiv\int_{-\infty}^{t}dt'\exp[-i\omega\tau+ik(y'-y)]\delta\hat{\phi}_k(x') \tag{36}$$

occurs in Eq. (34), where $x'(t')$ and $y'(t')$ are the particle orbits in the equilibrium field configuration [Eqs. (30) and (31)].

In Sec. IV, Eqs. (34)–(36) are analyzed for the specific choice of equilibrium distribution function $f_b^0(H,P_y)$ in Eq. (14). In this regard, it is useful to further simplify Eqs. (34) and (35) making use of the identity

$$\frac{\partial}{\partial p_y}(If_b^0)=f_b^0\frac{\partial I}{\partial p_y}+I\left[\frac{\partial f_b^0}{\partial P_y}+v_y\frac{\partial f_b^0}{\partial H}\right]\ , \tag{37}$$

where $\partial H/\partial p_y=p_y/m=v_y$. We substitute Eq. (34) into Eq. (35) and make use of Eq. (37) to eliminate $I\partial f_b^0/\partial P_y$. Integrating by parts with respect to p_y, Poisson's equation (35) can then be expressed in the equivalent form[17]

$$\frac{\partial^2}{\partial x^2}\delta\hat{\phi}_k(x)-k^2\delta\hat{\phi}_k(x)=4\pi e^2\int d^3p\left[f_b^0 ik\frac{\partial I}{\partial p_y}-i(\omega-kv_y)I\frac{\partial f_b^0}{\partial H}-\delta\hat{\phi}_k(x)\frac{\partial f_b^0}{\partial H}\right], \tag{38}$$

where the orbit integral I is defined in Eq. (36). As indicated earlier, in Sec. IV the eigenvalue equation (38) is analyzed in circumstances where the equilibrium distribution function is specified by $f_b^0(H,P_y)=(\hat{n}_b/2\pi m)\delta(H)\delta(P_y)$.

B. Particle trajectories in the equilibrium fields

In this section, we determine the particle trajectories $\mathbf{x}'(t')$ and $\mathbf{v}'(t')$ in the equilibrium field configuration corresponding to the rectangular density profile in Eq. (19) and Fig. 2 and the choice of equilibrium distribution function in Eq. (14). From Eq. (20) and $E_x^0(x)=-\partial\phi_0(x)/\partial x$, the equilibrium electric field within the electron layer is given by $E_x^0(x)=E_c-(m/e)\hat{\omega}_{pb}^2 x$ for $0\le x<x_b$. Eliminating E_c by means of Eq. (22), we obtain

$$E_x^0(x)=-\frac{m}{2e}(\omega_c^2-\hat{\omega}_{pb}^2)x_b-\frac{m}{e}\hat{\omega}_{pb}^2 x \tag{39}$$

for $0\le x<x_b$. From Eq. (30), the axial motion is free-streaming with $v_z'=v_z$ and $z'=z+v_z\tau$. Making use of Eqs. (30) and (39), the (x',y') motion is determined from

$$\frac{dv_x'}{dt'}=\tfrac{1}{2}(\omega_c^2-\hat{\omega}_{pb}^2)x_b+\hat{\omega}_{pb}^2 x'-\omega_c v_y' \tag{40}$$

and

$$\frac{dv_y'}{dt'}=\omega_c v_x' \tag{41}$$

within the electron layer ($0\le x<x_b$). Equation (41) can be integrated to give

$$v_y'-\omega_c x'=v_y-\omega_c x=P_y/m=\text{const}, \tag{42}$$

where use has been made of the boundary conditions $v_y'(t'=t)=v_y$ and $x'(t'=t)=x$. Eliminating v_y' in Eq. (40) by means of Eq. (42), we obtain the oscillator equation for $x'(t')$

$$\frac{d^2}{dt'^2}x'+(\omega_c^2-\hat{\omega}_{pb}^2)x'=\tfrac{1}{2}(\omega_c^2-\hat{\omega}_{pb}^2)x_b-\omega_c(v_y-\omega_c x)\ . \tag{43}$$

Equation (43) is solved subject to the boundary conditions $x'(t'=t)=x$ and $v_x'(t'=t)=(dx'/dt')_{t'=t}=v_x$. Defining the betatron frequency ω_v (including self-field effects) by

$$\omega_v^2=\omega_c^2-\hat{\omega}_{pb}^2\ , \tag{44}$$

we obtain

$$x'=x+\left[x-x_M+\frac{\omega_c P_y}{m\omega_v^2}\right][\cos(\omega_v\tau)-1]+\frac{v_x}{\omega_v}\sin(\omega_v\tau)\ , \tag{45}$$

and

$$v_x'=v_x\cos(\omega_v\tau)-\omega_v\left[x-x_M+\frac{\omega_c P_y}{m\omega_v^2}\right]\sin(\omega_v\tau)\ , \tag{46}$$

where $x_M\equiv x_b/2$. From Eqs. (42) and (45), the y' motion is given by $v_y'=\omega_c x'+P_y/m$, i.e.,

$$v_y'=\left[\omega_c x+\frac{P_y}{m}\right]+\omega_c\left[x-x_M+\frac{\omega_c P_y}{m\omega_v^2}\right][\cos(\omega_v\tau)-1]+\frac{\omega_c v_x}{\omega_v}\sin(\omega_v\tau) \tag{47}$$

and

$$y'=y+\left[\omega_c x_M-\frac{\hat{\omega}_{pb}^2 P_y}{m\omega_v^2}\right]\tau+\frac{\omega_c v_x}{\omega_v^2}[1-\cos(\omega_v\tau)]+\frac{\omega_c}{\omega_v}\left[x-x_M+\frac{\omega_c P_y}{m\omega_v^2}\right]\sin(\omega_v\tau)\ . \tag{48}$$

For future purposes of evaluating the $\partial I/\partial p_y$ term in the eigenvalue equation (38), we make use of Eqs. (45) and (48) to calculate $\partial x'/\partial p_y$ and $\partial y'/\partial p_y$. This gives

$$\frac{\partial x'}{\partial p_y}=\frac{\omega_c}{m\omega_v^2}[\cos(\omega_v\tau)-1]\ , \tag{49}$$

$$\frac{\partial y'}{\partial p_y}=-\frac{\hat{\omega}_{pb}^2}{m\omega_v^2}\tau+\frac{\omega_c^2}{m\omega_v^3}\sin(\omega_v\tau)\ . \tag{50}$$

Moreover, for electrons with $P_y=0$, the orbits (x_0',v_{x0}') and (y_0',v_{y0}') can be expressed as

$$\begin{aligned} x_0'&=x_M+(x-x_M)\cos(\omega_v\tau)+\frac{v_x}{\omega_v}\sin(\omega_v\tau)\ ,\\ v_{x0}'&=v_x\cos(\omega_v\tau)-\omega_v(x-x_M)\sin(\omega_v\tau)\ , \end{aligned} \tag{51}$$

and

$$\begin{aligned} y_0'&=y+\omega_c v_x/\omega_v^2+\omega_c x_M\tau-\frac{\omega_c v_x}{\omega_v^2}\cos(\omega_v\tau)+\frac{\omega_c}{\omega_v}(x-x_M)\sin(\omega_v\tau)\ ,\\ v_{y0}'&=\omega_c x_M+\omega_c(x-x_M)\cos(\omega_v\tau)+\frac{\omega_c v_x}{\omega_v}\sin(\omega_v\tau)\ . \end{aligned} \tag{52}$$

From Eq. (52), we note that the average (nonoscillatory) drift velocity in the y direction is given by

$$V_d=\omega_c x_M=\omega_c x_b/2 = -\frac{\omega_c e E_c}{m\omega_v^2} , \tag{53}$$

where use has been made of Eq. (22) to eliminate x_b. That is, the average y velocity is $\bar{v}'_{y0}=V_d$, where the overbar denotes average over the ω_v oscillations in Eq. (52). Similarly, $\bar{y}'_0=y+\omega_c v_x/\omega_v^2+V_d\tau$, and $(\bar{x}'_0,\bar{v}'_{x0})=(x_M,0)$. Note that the average orbit for x'_0 oscillates about $x_M=x_b/2$, which is the midway point between the cathode ($x=0$) and the boundary of the electron layer ($x=x_b$).

IV. ELECTROSTATIC EIGENVALUE EQUATION

A. Exact eigenvalue equation

In this section, we simplify the electrostatic eigenvalue equation (38) for the choice of equilibrium distribution function in Eq. (14) and rectangular density profile in Eq. (19) and Fig. 2. The corresponding particle trajectories (x',y'), required in evaluating the orbit integral I in Eq. (36), are defined in Eqs. (45) and (48). Substituting Eq. (14) into Eq. (38) and integrating over p_y, Poisson's equation can be expressed as

$$\frac{\partial}{\partial x^2}\delta\hat{\phi}_k(x)-k^2\delta\hat{\phi}_k(x)=4\pi e^2\int dp_x dp_z\frac{\hat{n}_b}{2\pi m}\left[\delta(H_0)ik\left[\frac{\partial I}{\partial p_y}\right]_0-[i(\omega-k\omega_c x)I_0+\delta\hat{\phi}_k(x)]\frac{\partial}{\partial H_0}\delta(H_0)\right] , \tag{54}$$

where $H_0\equiv[H]_{P_y=0}=(p_x^2+p_z^2)/2m-p_{\perp 0}^2(x)/2m$, the effective perpendicular momentum $p_{\perp 0}(x)$ is defined in Eq. (16), and I_0 and $(\partial I/\partial p_y)_0$ are defined by

$$I_0=[I]_{P_y=0}=\int_{-\infty}^{t}dt'\exp[-i\omega\tau+ik(y'_0-y)]\delta\hat{\phi}_k(x'_0) \tag{55}$$

and

$$\left[\frac{\partial I}{\partial p_y}\right]_0=\left[\frac{\partial I}{\partial p_y}\right]_{P_y=0}=\int_{-\infty}^{t}dt'\exp[-i\omega\tau+ik(y'_0-y)]\left[ik\left[-\frac{\hat{\omega}_{pb}^2}{m\omega_v^2}\tau+\frac{\omega_c^2}{m\omega_v^3}\sin(\omega_v\tau)\right]\delta\hat{\phi}_k(x'_0)+\frac{\omega_c}{m\omega_v^2}[\cos(\omega_v\tau)-1]\frac{\partial}{\partial x'_0}\delta\hat{\phi}_k(x'_0)\right] . \tag{56}$$

In Eqs. (55) and (56), (x'_0,y'_0) are the $P_y=0$ trajectories defined in Eqs. (51) and (52), and use has been made of Eqs. (49) and (50) in deriving Eq. (56).

The eigenvalue equation (54) and supporting definitions in Eqs. (51), (52), (55), and (56) constitute an exact description of the linear stability properties for electrostatic perturbations about the self-consistent kinetic equilibrium in Eq. (14). Equation (54) can, in principle, be simplified and analyzed in several parameter regimes of physical interest.

B. Approximate eigenvalue equation for $\omega\approx kV_d$

For present purposes, we assume $\hat{\omega}_{pb}^2<\omega_c^2$ and $\omega_v\neq 0$ and consider perturbations with frequency ω and wave number k satisfying[17]

$$|\omega-kV_d|\ll\omega_v . \tag{57}$$

That is, the wave perturbation has phase velocity ω/k nearly synchronous with the average particle drift velocity V_d in the y direction. Moreover, the Doppler-shifted frequency $\omega-kV_d$ is far removed from resonance with the betatron frequency ω_v defined in Eq. (44). In addition, it is assumed that the perturbation wavelength in the y direction is long with[17]

$$kx_M\ll 1 , \tag{58}$$

and that the x variation of the eigenfunction $\delta\hat{\phi}_k(x)$ is sufficiently slow that $|x_M\partial/\partial x|\lesssim 1$. In the present analysis, we adopt a model in which all oscillatory contribution to x'_0 and y'_0 in Eqs. (55) and (56) are neglected [see Eqs. (51) and (52)]. These terms generally give rise to harmonic contributions to the exponent in the orbit integral (55) of the form $\omega-kV_d-n\omega_v$ for $n\neq 0$, as well as a modification of the amplitude of the $n=0$ term in the orbit integral proportional to $(\omega-kV_d)^{-1}$. Specifically, in order to investigate the qualitative features of stability properties for $|\omega-kV_d|\ll\omega_v$ and $kx_M\ll 1$, the model approximates $y'_0=y+V_d\tau$, $x'_0=x_M$, $\delta\hat{\phi}_k(x'_0)=\delta\hat{\phi}_k(x_M)$, and

$$(\partial/\partial x'_0)\delta\hat{\phi}_k(x'_0)=[\partial\delta\hat{\phi}_k(x)/\partial x]_{x=x_M}$$

in Eqs. (55) and (56). This gives

$$I_0=\int_{-\infty}^{t}dt'\exp(-i\omega\tau+ikV_d\tau)\delta\hat{\phi}_k(x_M)=i\frac{\delta\hat{\phi}_k(x_M)}{\omega-kV_d} \tag{59}$$

and

$$\left[\frac{\partial I}{\partial p_y}\right]_0 = \int_{-\infty}^{t} dt' \exp(-i\omega\tau + ikV_d\tau)\left[-i\frac{k\mu}{m}\tau\delta\hat{\phi}_k(x_M) - \frac{\omega_c}{m\omega_v^2}\frac{\partial}{\partial x_M}\delta\hat{\phi}_k(x_M)\right]$$

$$= -\frac{ik\mu}{m}\frac{\delta\hat{\phi}_k(x_M)}{(\omega - kV_d)^2} - i\frac{\omega_c}{m\omega_v^2}\frac{1}{\omega - kV_d}\left[\frac{\partial}{\partial x}\delta\hat{\phi}_k\right]_{x=x_M} . \tag{60}$$

In Eq. (60), we have introduced the quantity μ defined by

$$\mu = \frac{\omega_c^2}{\omega_v^2} - 1 = \frac{\hat{\omega}_{pb}^2}{\omega_v^2} . \tag{61}$$

Note that μ is a measure of the strength of the equilibrium self-electric field. For $\hat{\omega}_{pb}^2 \ll \omega_c^2$, it follows that $\mu \simeq \hat{\omega}_{pb}^2/\omega_c^2 \ll 1$, corresponding to weak self-electric field. On the other hand, for $\hat{\omega}_{pb}^2/\omega_c^2 = 0.5$ (say), it follows that $\mu = 1$, and the self-electric field is much stronger than for the case of a tenuous electron layer.

Substituting the approximate expressions (59) and (60) into Eq. (54), the eigenvalue equation becomes

$$\frac{\partial^2}{\partial x^2}\delta\hat{\phi}_k(x) - k^2\delta\hat{\phi}_k(x) = \hat{\omega}_{pb}^2\left[k^2\mu\frac{\delta\hat{\phi}_k(x_M)}{(\omega - kV_d)^2} + \frac{\omega_c}{\omega_v^2}\frac{k}{\omega - kV_d}\left[\frac{\partial}{\partial x}\delta\hat{\phi}_k\right]_{x=x_M}\right]\int \frac{dp_x dp_z}{2\pi m}\delta(H_0)$$

$$-\hat{\omega}_{pb}^2\left[-\frac{\omega - k\omega_c x}{\omega - kV_d}\delta\hat{\phi}_k(x_M) + \delta\hat{\phi}_k(x)\right]\int \frac{dp_x dp_z}{2\pi}\frac{\partial}{\partial H_0}\delta(H_0) . \tag{62}$$

Paralleling the evaluation of the equilibrium density profile $n_b^0(x)$ in Sec. II C, it is straightforward to show that the contribution in Eq. (62) proportional to $(2\pi m)^{-1}\int dp_x dp_z \delta(H_0)$ corresponds to a body-charge perturbation extending from $x=0$ to $x=x_b$, whereas the term proportional to $(2\pi)^{-1}\int dp_x dp_z(\partial/\partial H_0)\delta(H_0)$ corresponds to a surface-charge perturbation at $x=x_b$. Making use of $2mH_0 = p_\perp^2 - p_{\perp 0}^2(x)$, where $p_\perp^2 = p_x^2 + p_z^2$ and $p_{\perp 0}^2(x) = m^2\omega_v^2 x(x_b - x)$, we obtain

$$\int \frac{dp_x dp_z}{2\pi m}\delta(H_0) = \int_0^\infty dp_\perp^2 \delta(p_\perp^2 - p_{\perp 0}^2) = U(x_b - x) \tag{63}$$

for $x \geq 0$. Here, $U(x_b - x)$ is the Heaviside step function defined by $U(x_b - x) = +1$ for $x < x_b$ and $U(x_b - x) = 0$ for $x > x_b$. Similarly, it is readily shown that

$$\int \frac{dp_x dp_z}{2\pi}\frac{\partial}{\partial H_0}\delta(H_0) = 2m^2\int_0^\infty dp_\perp^2 \frac{\partial}{\partial p_\perp^2}\delta(p_\perp^2 - p_{\perp 0}^2)$$

$$= -\frac{2}{\omega_v^2 x_b}\delta(x - x_b) . \tag{64}$$

Substituting Eqs. (63) and (64) into Eq. (62), the eigenvalue equation becomes (for $0 \leq x \leq d$)

$$\frac{\partial^2}{\partial x^2}\delta\hat{\phi}_k(x) - k^2\delta\hat{\phi}_k(x) = \hat{\omega}_{pb}^2\left[k^2\mu\frac{\delta\hat{\phi}_k(x_M)}{(\omega - kV_d)^2} + \frac{\omega_c}{\omega_v^2}\frac{k}{\omega - kV_d}\left[\frac{\partial}{\partial x}\delta\hat{\phi}_k\right]_{x=x_M}\right]U(x_b - x)$$

$$+\frac{\mu}{x_M}\left[[\delta\hat{\phi}_k(x) - \delta\hat{\phi}_k(x_M)] + \frac{k\omega_c(x - x_M)}{\omega - kV_d}\delta\hat{\phi}_k(x_M)\right]\delta(x - x_b) , \tag{65}$$

where use has been made of $x_M = x_b/2$, $\mu = \hat{\omega}_{pb}^2/\omega_v^2$, and $V_d = \omega_c x_M$.

The simplified eigenvalue equation (65) can be solved exactly (Sec. IV C) for the eigenfunction $\delta\hat{\phi}_k(x)$ and complex eigenfrequency ω. Keep in mind that Eq. (65) is valid for $|\omega - kV_d|^2 \ll \omega_v^2$ and $kx_b \ll 1$ [Eqs. (57) and (58)].

C. Solution to approximate eigenvalue equation

Within the electron layer ($0 \leq x < x_b$), only the body-charge perturbation proportional to $U(x_b - x)$ contributes on the right-hand side of Eq. (65). On the other hand, in the region $x_b < x \leq d$, Eq. (65) reduces to the vacuum eigenvalue equation $(\partial^2/\partial x^2)\delta\hat{\phi}_k - k^2\delta\hat{\phi}_k = 0$. Therefore, the solution to Eq. (65) that satisfies $\delta\hat{\phi}_k(x=0) = 0 = \delta\hat{\phi}_k(x=d)$ can be expressed as

$$\delta\hat{\phi}_k(x)=\begin{cases} A\sinh(kx)+B[\cosh(kx)-1], & 0\le x<x_b \\ \dfrac{[A\sinh(kx_b)+B[\cosh(kx_b)-1]}{\sinh[k(x_b-d)]}\sinh[k(x-d)], & x_b<x\le d \end{cases} \tag{66}$$

where we have enforced continuity of $\delta\hat{\phi}_k(x)$ at $x=x_b$. Substituting Eq. (66) into Eq. (65), the coefficient B is given by

$$B=\frac{\hat{\omega}_{pb}^2}{k^2}\left[k^2\mu\frac{\delta\hat{\phi}_k(x_M)}{(\omega-kV_d)^2}+\frac{\omega_c}{\omega_v^2}\frac{k}{\omega-kV_d}\left[\frac{\partial}{\partial x}\delta\hat{\phi}_k\right]_{x=x_M}\right] . \tag{67}$$

Moreover, integrating Eq. (65) across the surface of the electron layer at $x=x_b$, we find

$$\lim_{\epsilon\to 0_+}\left[\frac{\partial}{\partial x}\delta\hat{\phi}_k\bigg|_{x_b+\epsilon}-\frac{\partial}{\partial x}\delta\hat{\phi}_k\bigg|_{x_b-\epsilon}\right]=\frac{\mu}{x_M}\left[[\delta\hat{\phi}_k(x_b)-\delta\hat{\phi}_k(x_M)]+\frac{kV_d}{\omega-kV_d}\delta\hat{\phi}_k(x_M)\right] , \tag{68}$$

where use has been made of $\omega_c(x_b-x_M)=\omega_c x_M=V_d$. Substituting Eq. (66) into Eq. (68) gives

$$k[A\cosh(kx_b)+B\sinh(kx_b)]-k\{A\sinh(kx_b)+B[\cosh(kx_b)-1]\}\frac{\cosh[k(x_b-d)]}{\sinh[k(x_b-d)]} =\frac{\mu}{x_M}\left[[\delta\hat{\phi}_k(x_b)-\delta\hat{\phi}_k(x_M)]+\frac{kV_d}{\omega-kV_d}\delta\hat{\phi}_k(x_M)\right] , \tag{69}$$

which relates the discontinuity in perturbed electric field at $x=x_b$ to the perturbed surface-charge density.

From Eq. (66), we find that $\delta\hat{\phi}_k(x_M)$, $(\partial\delta\hat{\phi}_k/\partial x)_{x=x_M}$, and $\delta\hat{\phi}_k(x_b)$ can be expressed in terms of A, B, kx_b, and kx_M by

$$\delta\hat{\phi}_k(x_M)=A\sinh(kx_M)+B[\cosh(kx_M)-1] , \tag{70}$$

$$\left[\frac{\partial}{\partial x}\delta\hat{\phi}_k\right]_{x=x_M}=kA\cosh(kx_M)+kB\sinh(kx_M) , \tag{71}$$

and

$$\delta\hat{\phi}_k(x_b)=A\sinh(kx_b)+B[\cosh(kx_b)-1] . \tag{72}$$

Substituting Eqs. (70) and (71) into the definition of B in Eq. (67) gives

$$A\left[\mu\frac{\hat{\omega}_{pb}^2}{(\omega-kV_d)^2}\sinh(kx_M)+\mu\frac{\omega_c}{(\omega-kV_d)}\cosh(kx_M)\right] +B\left[\mu\frac{\hat{\omega}_{pb}^2}{(\omega-kV_d)^2}[\cosh(kx_M)-1]-1+\mu\frac{\omega_c}{\omega-kV_d}\sinh(kx_M)\right]=0 , \tag{73}$$

which relates the coefficients A and B. The second independent relation between A and B is obtained by substituting Eqs. (70) and (72) on the right-hand side of Eq. (69). This gives

$$A\left[kx_M\cosh(kx_b)-\sinh(kx_b)\{kx_M\coth[k(x_b-d)]-\mu\}-\mu\frac{\omega-2kV_d}{\omega-kV_d}\sinh(kx_M)\right] +B\left[kx_M\sinh(kx_b)-[\cosh(kx_b)-1]\{kx_M\coth[k(x_b-d)]-\mu\}-\mu\frac{\omega-2kV_d}{\omega-kV_d}[\cosh(kx_M)-1]\right]=0 . \tag{74}$$

The dispersion relation that determines the complex eigenfrequency ω in terms of equilibrium parameters and the wave number k is obtained by setting the determinant of the coefficients of A and B in Eqs. (73) and (74) equal to zero.

D. Analysis of electrostatic dispersion relation

We expand the coefficients of A and B in Eqs. (73) and (74) for $kx_b \ll 1$ [Eq. (58)]. Retaining leading-order terms and setting the determinant of the coefficients of A and B in Eqs. (73) and (74) equal to zero gives

$$\mu\frac{kV_d}{\omega-kV_d}\left[1+\frac{\hat{\omega}_{pb}^2}{\omega_c^2}\frac{kV_d}{\omega-kV_d}\right]\left[1+\frac{d}{d-x_b}+\frac{3}{2}\mu+\frac{\mu}{2}\frac{kV_d}{\omega-kV_d}\right]$$
$$=-\left[1-\mu\frac{kV_d}{\omega-kV_d}-\frac{\mu}{2}\frac{\hat{\omega}_{pb}^2}{\omega_c^2}\frac{k^2V_d^2}{(\omega-kV_d)^2}\right]\left[\frac{d}{d-x_b}+\mu+\mu\frac{kV_d}{\omega-kV_d}\right], \quad (75)$$

where use has been made of $x_b=2x_M$ and $V_d=\omega_c x_M$. Introducing the dimensionless frequency Ω defined by

$$\Omega=\frac{\omega-kV_d}{kV_d}, \quad (76)$$

the dispersion relation (75) can be expressed in the equivalent form

$$\left[\frac{d}{d-x_b}+\mu\right]\Omega^2+2\mu(1+\tfrac{1}{4}\mu)\Omega+\frac{1}{2}\frac{\mu^2}{1+\mu}\left[1+\mu+\frac{d}{d-x_b}\right]=0, \quad (77)$$

where use has been made of $\hat{\omega}_{pb}^2/\omega_c^2=\mu/(1+\mu)$.

Equation (77) is the final dispersion relation within the context of the present simplified model based on the assumptions in Eqs. (57) and (58). As such, no *a priori* approximation has been made that the electron density is low ($\mu\ll 1$). Indeed, Eq. (77) is valid even if the parameter $\mu=\hat{\omega}_{pb}^2/\omega_v^2$ is of order unity or larger, as long as the betatron frequency ω_v does not become so small that the inequality in Eq. (57) is violated.

The quadratic dispersion relation (77) can be solved exactly for the complex normalized eigenfrequency $\Omega=(\omega-kV_d)/kV_d$. Introducing the geometric factor

$$g=\frac{d}{d-x_b}, \quad (78)$$

the necessary and sufficient condition for instability ($\mathrm{Im}\omega>0$) obtained from Eq. (77) can be expressed as

$$\frac{1}{2}\frac{(1+\mu+g)(\mu+g)}{(1+\mu)}>(1+\tfrac{1}{4}\mu)^2. \quad (79)$$

Equivalently, since $g=d/(d-x_b)>1$, Eq. (79) gives

$$g>[\tfrac{1}{4}(3+2\mu)^2+\tfrac{1}{8}\mu^2(1+\mu)]^{1/2}-\tfrac{1}{2}(1+2\mu) \quad (80)$$

as the necessary and sufficient condition for instability. For the case of moderately low electron density satisfying $\mu\lesssim 1$, Eq. (80) can be approximated by

$$g>1+\frac{\mu^2(1+\mu)}{8(3+2\mu)}. \quad (81)$$

When the inequality in Eq. (80) is satisfied, the real oscillation frequency ($\mathrm{Re}\omega$) and growth rate ($\mathrm{Im}\omega$) determined from Eq. (77) are given by (for $kV_d>0$)

$$\mathrm{Re}\omega-kV_d=-kV_d\frac{\mu}{(g+\mu)}\left[1+\frac{\mu}{4}\right], \quad (82)$$

and

$$\mathrm{Im}\omega=kV_d\frac{\mu}{g+\mu}\times\left[\frac{1}{2}(g+\mu)\left[1+\frac{g}{1+\mu}\right]-\left[1+\frac{\mu}{4}\right]^2\right]^{1/2}. \quad (83)$$

Eliminating μ in favor of $\hat{\omega}_{pb}^2/\omega_c^2$, and introducing the parameter h defined by

$$h=\left[\frac{(3-\hat{\omega}_{pb}^2/\omega_c^2)^2}{4(1-\hat{\omega}_{pb}^2/\omega_c^2)^2}+\frac{\hat{\omega}_{pb}^4/\omega_c^4}{8(1-\hat{\omega}_{pb}^2/\omega_c^2)^3}\right]^{1/2}-\frac{1+\hat{\omega}_{pb}^2/\omega_c^2}{2(1-\hat{\omega}_{pb}^2/\omega_c^2)}, \quad (84)$$

the instability criterion in Eq. (80) can be expressed in the equivalent form

$$\frac{x_b}{d}>\frac{h-1}{h}. \quad (85)$$

Stability boundaries in the parameter space (μ,g) are illustrated in Fig. 3. The solid curve corresponds to the stability boundary ($\mathrm{Im}\omega=0$) obtained from Eq. (80), whereas the dashed curve corresponds to the stability boundary obtained from the approximate criterion in Eq. (81). The region of (μ,g) parameter space *above* the curve corresponds to instability ($\mathrm{Im}\omega>0$), whereas the region of parameter space *below* the curve corresponds to stable oscillations ($\mathrm{Im}\omega=0$). As expected, the approximate instability criterion in Eq. (81) is quite accurate for moderately

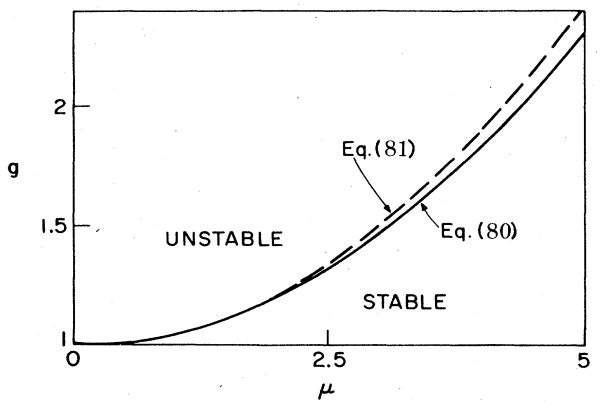

FIG. 3. Stability boundary in (μ,g) parameter space obtained from Eq. (80) (solid curve) and from Eq. (81) (dashed curve).

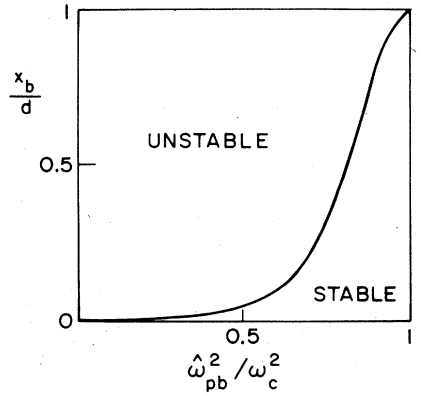

FIG. 4. Stability boundary in $(\hat{\omega}_{pb}^2/\omega_c^2, x_b/d)$ parameter space obtained from Eq. (85).

low electron density ($\mu \lesssim 1$). Shown in Fig. 4 is the stability boundary in the parameter space $(\hat{\omega}_{pb}^2/\omega_c^2, x_b/d)$ obtained from Eq. (85). We remind the reader that the stability analysis in Sec. IV has been restricted to low-frequency perturbations satisfying $|\omega - kV_d| \ll \omega_v = (\omega_c^2 - \hat{\omega}_{pb}^2)^{1/2}$ [Eq. (57)]. In this regard, the stability boundary obtained from Eq. (85) and illustrated in Fig. 4 is not valid as $\hat{\omega}_{pb}^2/\omega_c^2$ approaches unity.[6,7]

The normalized growth rate $(\mathrm{Im}\omega)/kV_d$ and real oscillation frequency $(\mathrm{Re}\omega - kV_d)/kV_d$ have been obtained from Eq. (77) for a broad range of system parameters μ and g. Shown in Fig. 5 are plots of the growth rate (dashed curve) and real oscillation frequency (solid curve) versus μ for the case $d = 2x_b$ and $g = 2$. Evidently, for the choice of parameters in Fig. 5, the growth rate assumes a maximum value of $(\mathrm{Im}\omega)_{\max} \simeq 0.5kV_d$ for $\mu \simeq 2.3$. Note also from Eq. (83) and Fig. 5 that $(\mathrm{Im}\omega)/kV_d$ increases linearly with μ for small μ, i.e.,

$$\frac{\mathrm{Im}\omega}{kV_d} \simeq \frac{\mu}{g}\left[\tfrac{1}{2}g(1+g)-1\right]^{1/2} \tag{86}$$

for $\mu \ll 1$. As expected from Fig. 3, it is found that instability ceases $(\mathrm{Im}\omega = 0)$ once μ exceeds some critical value (Fig. 5).

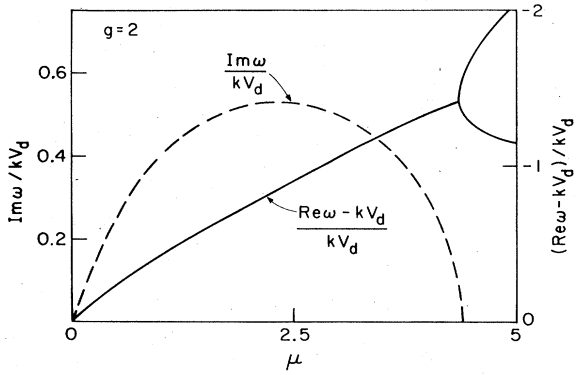

FIG. 5. Plot of normalized growth rate and real oscillation frequency vs μ obtained from Eq. (77) for $d = 2x_b$ and $g = 2$.

To summarize, within the context of the assumptions of low frequency [$|\omega - kV_d| \ll \omega_v$ in Eq. (57)] and long wavelength [$kx_M \ll 1$ in Eq. (58)], the kinetic stability analysis in Secs. III and IV leads to the approximate dispersion relation (77) for the complex eigenfrequency ω. The necessary and sufficient condition for instability $(\mathrm{Im}\omega > 0)$ is given in Eq. (80) and is illustrated in Figs. 3 and 4. It is clear that the maximum growth rate for instability can be substantial. For example, for the parameters in Fig. 5, $(\mathrm{Im}\omega)_{\max} \simeq 0.5kV_d = (0.5)(kx_M)\omega_c$, where $kx_M \ll 1$ has been assumed in Eq. (58).

V. CONCLUSIONS

In this paper, we have made use of the linearized Vlasov-Poisson equations to investigate the electrostatic stability properties of nonrelativistic nonneutral electron flow in a planar diode (Secs. II–IV). The detailed stability analysis has been carried out for flute perturbations $(\partial/\partial z = 0)$ about the choice of equilibrium distribution function $f_b^0(H,P_y) = (\hat{n}_b/2\pi m)\delta(H)\delta(P_y)$ in Eq. (14) with corresponding self-consistent rectangular density profile $n_b^0(x)$ in Eq. (19) and parabolic temperature profile $T_{\perp b}^0(x)$ in Eq. (25) (see also Fig. 2). For low-frequency [Eq. (57)], long-wavelength [Eq. (58)] perturbations, the eigenvalue equation is approximated by Eq. (65), and the corresponding dispersion relation for the complex eigenfrequency ω is given by Eq. (77). The detailed analysis of Eq. (77) in Sec. IV D shows that instability exists $(\mathrm{Im}\omega > 0)$ for the region of (μ,g) parameter space defined in Eq. (80) and illustrated in Fig. 3. Moreover, the analysis indicates that the maximum growth rate of the instability can be substantial, depending on the values of μ and g.

Finally, the analysis in Sec. IV D emphasizes stability behavior in a parameter regime corresponding to instability $(\mathrm{Im}\omega > 0)$. A further important property readily follows from the analysis of the dispersion relation (77). Namely, the inequality

$$\mu > \mu_M(g) \tag{87}$$

is a necessary and sufficient condition for stability, where $\mu_M(g)$ is the solution to [see Eq. (83)]

$$(\mu_M+g)(1+\mu_M+g) = 2(1+\mu_M)\left[1+\frac{\mu_M}{4}\right]^2 . \tag{88}$$

That is, Eq. (77) supports only purely oscillatory solutions $(\mathrm{Im}\omega = 0)$ when the inequality in Eq. (87) is satisfied (Fig. 3). Making use of $\mu = \hat{\omega}_{pb}^2/(\omega_c^2 - \hat{\omega}_{pb}^2)$, Eq. (87) can be expressed in the equivalent form

$$\frac{\hat{\omega}_{pb}^2}{\omega_c^2} > \frac{\mu_M}{1+\mu_M} . \tag{89}$$

That is, at sufficiently high density, the instability described in Sec. IV D is completely stabilized (Fig. 4). Since $\mu_M/(1+\mu_M) < 1$, we note from Eq. (89) that stabili-

zation occurs at densities below the condition for Brillouin flow. For example, for $d=2x_b$ and $g=2$, Eq. (89) gives $\hat{\omega}_{pb}^2/\omega_c^2 \gtrsim 0.8$ as the condition for stability. This may have important implications for stable diode operation. In particular, if the density buildup of the electron layer is such that $\hat{\omega}_{pb}^2/\omega_c^2$ exceeds $\mu_M/(1+\mu_M)$ on a sufficiently fast time scale, then the instability discussed in Sec. IV D need not have a deleterious effect on electron layer stability and confinement.

ACKNOWLEDGMENTS

This research was supported by Sandia National Laboratories and in part by the Office of Naval Research.

[1]R. C. Davidson and K. Tsang, Phys. Rev. A **29**, 488 (1984).
[2]H. S. Uhm and R. C. Davidson, Phys. Rev. A **31**, 2556 (1985).
[3]R. C. Davidson, Phys. Fluids **28**, 1937 (1985).
[4]R. C. Davidson, K. Tsang, and J. Swegle, Phys. Fluids **27**, 2332 (1984).
[5]R. C. Davidson, Phys. Fluids **28**, 377 (1985).
[6]J. Swegle, Phys. Fluids **26**, 1670 (1983).
[7]J. Swegle and E. Ott, Phys. Fluids **24**, 1821 (1981).
[8]J. P. VanDevender, J. P. Quintenz, R. J. Leeper, D. J. Johnson, and J. T. Crow, J. Appl. Phys. **52**, 4 (1981).
[9]R. B. Miller, *Intense Charged Particle Beams* (Plenum, New York, 1982).
[10]R. H. Levy, Phys. Fluids **8**, 1288 (1965).
[11]O. Buneman, R. H. Levy, and L. M. Linson, J. Appl. Phys. **37**, 3203 (1966).
[12]R. J. Briggs, J. D. Daugherty, and R. H. Levy, Phys. Fluids **13**, 421 (1970).
[13]R. C. Davidson, *Theory of Nonneutral Plasmas* (Benjamin, Reading, Mass., 1974), Chap. 2.
[14]V. S. Voronen and A. N. Lebedev, Zh. Tekh. Fiz. **43**, 2591 (1973) [Sov. Phys.—Tech. Phys. **18**, 1627 (1974)].
[15]E. Ott and R. V. Lovelace, Appl. Phys. Lett. **27**, 378 (1975).
[16]R. C. Davidson, *Theory of Nonneutral Plasmas,* Ref. 13, Chap. 3.
[17]R. C. Davidson, H. S. Uhm, and S. M. Mahajan, Phys. Fluids **19**, 1608 (1976).
[18]H. S. Uhm and R. C. Davidson, Phys. Fluids **20**, 771 (1977).
[19]R. C. Davidson and N. A. Krall, Phys. Fluids **13**, 1543 (1970).
[20]A. Nocentini, H. L. Berk, and R. N. Sudan, J. Plasma Phys. **2**, 311 (1968).
[21]J. M. Creedon, J. Appl. Phys. **48**, 1070 (1977).
[22]C. W. Mendel, Jr., D. B. Seidel, and S. E. Rosenthal, Laser and Particle Beam Fusion **1**, 311 (1983).